Upper limit on the decay $\Sigma(1385)^- \to \Sigma^-\gamma$, and cross section for $\gamma\Sigma^- \to \Lambda\pi^-$

The SELEX Collaboration

V.V. Molchanov [f,*], G. Alkhazov [k], A.G. Atamantchouk [k,1],
M.Y. Balatz [h,1], N.F. Bondar [k], D. Casey [r], P.S. Cooper [e],
L.J. Dauwe [q], G.V. Davidenko [h], U. Dersch [i,2],
A.G. Dolgolenko [h], G.B. Dzyubenko [h], R. Edelstein [c],
L. Emediato [t], A.M.F. Endler [d], J. Engelfried [m,e], I. Eschrich [i,3],
C.O. Escobar [t,4], A.V. Evdokimov [h], T. Ferbel [r],
I.S. Filimonov [j,1], F.G. Garcia [t,e], M. Gaspero [s], I. Giller [ℓ],
V.L. Golovtsov [k], P. Gouffon [t], E. Gülmez [b], C. Hammer [r],
He Kangling [g], M. Iori [s], S.Y. Jun [c], M. Kaya [p,5], J. Kilmer [e],
V.T. Kim [k], L.M. Kochenda [k], I. Konorov [i,6],
A.P. Kozhevnikov [f], A.G. Krivshich [k], H. Krüger [i,7],
M.A. Kubantsev [h], V.P. Kubarovsky [f], A.I. Kulyavtsev [c,e],
N.P. Kuropatkin [k,e], V.F. Kurshetsov [f], A. Kushnirenko [c],
S. Kwan [e], J. Lach [e], A. Lamberto [u], L.G. Landsberg [f], I. Larin [h],
E.M. Leikin [j], Li Yunshan [g], M. Luksys [n], T. Lungov [t],
V.P. Maleev [k], D. Mao [c,8], Mao Chensheng [g], Mao Zhenlin [g],
P. Mathew [c,9], M. Mattson [c], V. Matveev [h], E. McCliment [p],
M.A. Moinester [ℓ], A. Morelos [m], V.A. Mukhin [f],
K.D. Nelson [p,10], A.V. Nemitkin [j], P.V. Neoustroev [k],
C. Newsom [p], A.P. Nilov [h], S.B. Nurushev [f], A. Ocherashvili [ℓ,11],
Y. Onel [p], E. Ozel [p], S. Ozkorucuklu [p,12], A. Penzo [u],
S.V. Petrenko [f], P. Pogodin [p], M. Procario [c,13], V.A. Prutskoi [h],
E. Ramberg [e], G.F. Rappazzo [u], B.V. Razmyslovich [k,14],
V.I. Rud [j], J. Russ [c], P. Schiavon [u], J. Simon [i,15], A.I. Sitnikov [h],
D. Skow [e], P. Slattery [r], V.J. Smith [o], M. Srivastava [t],
V. Steiner [ℓ], V. Stepanov [k,14], L. Stutte [e], M. Svoiski [k,14],
N.K. Terentyev [k,c], G.P. Thomas [a], L.N. Uvarov [k],
A.N. Vasiliev [f], D.V. Vavilov [f], V.S. Verebryusov [h],
V.A. Victorov [f], V.E. Vishnyakov [h], A.A. Vorobyov [k],

K. Vorwalter [i,16], J. You [c,e], Zhao Wenheng [g], Zheng Shuchen [g],
Z.H. Zhu [r], M. Zielinski [r], R. Zukanovich-Funchal [t]

[a]*Ball State University, Muncie, IN 47306, U.S.A.*
[b]*Bogazici University, Bebek 80815 Istanbul, Turkey*
[c]*Carnegie-Mellon University, Pittsburgh, PA 15213, U.S.A.*
[d]*Centro Brasileiro de Pesquisas Físicas, Rio de Janeiro, Brazil*
[e]*Fermi National Accelerator Laboratory, Batavia, IL 60510, U.S.A.*
[f]*Institute for High Energy Physics, Protvino, Russia*
[g]*Institute of High Energy Physics, Beijing, P.R. China*
[h]*Institute of Theoretical and Experimental Physics, Moscow, Russia*
[i]*Max-Planck-Institut für Kernphysik, 69117 Heidelberg, Germany*
[j]*Moscow State University, Moscow, Russia*
[k]*Petersburg Nuclear Physics Institute, St. Petersburg, Russia*
[ℓ]*Tel Aviv University, 69978 Ramat Aviv, Israel*
[m]*Universidad Autónoma de San Luis Potosí, San Luis Potosí, Mexico*
[n]*Universidade Federal da Paraíba, Paraíba, Brazil*
[o]*University of Bristol, Bristol BS8 1TL, United Kingdom*
[p]*University of Iowa, Iowa City, IA 52242, U.S.A.*
[q]*University of Michigan-Flint, Flint, MI 48502, U.S.A.*
[r]*University of Rochester, Rochester, NY 14627, U.S.A.*
[s]*University of Rome "La Sapienza" and INFN, Rome, Italy*
[t]*University of São Paulo, São Paulo, Brazil*
[u]*University of Trieste and INFN, Trieste, Italy*

Abstract

Coherent $\Lambda\pi^-$ production on Pb of $600\,\mathrm{GeV}$ Σ^- hyperons has been studied with the SELEX facility at Fermilab. Using the Primakoff formalism, we set a 90% CL upper limit on the radiative decay width $\Gamma[\Sigma(1385)^- \to \Sigma^-\gamma] < 9.5\,\mathrm{keV}$, and estimate the cross section for $\gamma\Sigma^- \to \Lambda\pi^-$ at $\sqrt{s} \approx 1.385\,\mathrm{GeV}$ to be $56 \pm 16\,\mu\mathrm{b}$.

Key words: Hyperon radiative decay, Primakoff effect
PACS: 13.30.Ce, 13.40.Hq, 14.20.Jn

1 Introduction

Radiative decays of hadrons and other electromagnetic processes play an important role in the phenomenology of high energy physics. Interactions of real and virtual photons with electric charges of quark fields provide unique information about the quark content of hadrons and about phenomenological parameters such as form factors, magnetic moments, polarizabilities, etc. Being simpler to analyze than purely hadronic phenomena, such processes serve as a good testing ground for models of hadrons.

A lot of data is available on radiative decays of mesons [1]. Electromagnetic properties of the N and Δ baryons have also been studied extensively in resonance photoproduction and electroproduction reactions [2]. However, experimental data on radiative decays of hyperons (we do not include *weak* radiative decays) are rather scarce [3]. Only $\Sigma^0 \to \Lambda\gamma$ and $\Lambda(1520) \to \Lambda\gamma$ decays have been measured thus far. There are also indirect model-dependent estimates for $\Lambda(1405) \to \Lambda/\Sigma^0\gamma$ decays, based on the study of radiative capture of kaons in K^--mesonic atoms. No other radiative decays of hyperons have been observed, and previous upper limits are not very sensitive [4, 5].

Electromagnetic decays $\Sigma(1385)^- \to \Sigma^-\gamma$ and $\Xi(1530)^- \to \Xi^-\gamma$ are of particular interest. In the limit of unbroken SU(3) symmetry, these decays are forbidden by U-spin conservation [6]. Consequently, their observation could provide information on the SU(3) breaking mechanism. The decay $\Sigma(1385)^- \to \Sigma^-\gamma$ has been considered in the framework of SU(3) and SU(6) symmetry-breaking

* Corresponding author.
  Email address: `molchanov@mx.ihep.su` (V.V. Molchanov).
[1] deceased
[2] Present address: Infinion, München, Germany
[3] Present address: University of California at Irvine, Irvine, CA 92697, USA
[4] Present address: Instituto de Física da Universidade Estadual de Campinas, UNICAMP, SP, Brazil
[5] Present address: Kafkas University, Kars, Turkey
[6] Present address: Physik-Department, Technische Universität München, 85748 Garching, Germany
[7] Present address: The Boston Consulting Group, München, Germany
[8] Present address: Lucent Technologies, Naperville, IL
[9] Present address: SPSS Inc., Chicago, IL
[10] Present address: University of Alabama at Birmingham, Birmingham, AL 35294
[11] Present address: Imadent Ltd., Rehovot 76702, Israel
[12] Present address: Süleyman Demirel Universitesi, Isparta, Turkey
[13] Present address: DOE, Germantown, MD
[14] Present address: Solidum, Ottawa, Ontario, Canada
[15] Present address: Siemens Medizintechnik, Erlangen, Germany
[16] Present address: Allianz Insurance Group IT, München, Germany

schemes [6, 7, 8], in the nonrelativistic quark model of Isgur and Karl [9], the MIT bag model [10], Skyrme model [11, 12, 13], heavy baryon chiral perturbation theory [14, 15], quenched lattice calculations [16], and in other treatments [17, 18, 19]. Predictions for the radiative width vary from 1 to 9.5 keV, although most models predict a width of less than 4 keV.

The direct decay of $\Sigma(1385)^- \to \Sigma^- \gamma$ is difficult to measure because of its small partial width and high background from the $\Sigma(1385)^- \to \Sigma^- \pi^0$ decay with one lost photon. However, the width for this and many other decays of the type $a \to h + \gamma$ can be measured in the inverse reaction of coherent electromagnetic production in the Coulomb field of atomic nuclei

$$h + (A, Z) \to a + (A, Z) \tag{1}$$

The cross section for such reactions is proportional to the radiative decay width $\Gamma(a \to h + \gamma)$. Thus $\Gamma(a \to h + \gamma)$ can be determined by measuring the absolute cross section of the Coulomb contribution to Reaction (1). This method was proposed initially by Primakoff, Pomeranchuk and Shmushkevich [20, 21], and is usually referred to as the Primakoff effect. Detailed description of the method may be found in many review papers [22] and references therein.

In this Letter, we present results of a search for the Coulomb production reaction

$$\begin{aligned} \Sigma^- + \mathrm{Pb} &\to \Sigma(1385)^- + \mathrm{Pb} \\ &\quad\, \hookrightarrow \Lambda \pi^- \end{aligned} \tag{2}$$

at a beam energy of approximately 600 GeV in an experiment using the SELEX spectrometer (E781) at Fermilab.

2 Experimental apparatus

The SELEX facility [23] is a forward magnetic spectrometer with scintillation counters and hodoscopes, proportional and drift chambers, silicon microstrip beam and vertex detectors, additional downstream microstrip stations in the beam region, three lead glass photon detectors, a hadron calorimeter, two transition radiation detectors (TRD), and a multiparticle RICH counter.

The experiment was designed mainly to study production and decays of charm baryons in a hyperon beam [24]. It emphasized the forward production ($x_{\mathrm{F}} > 0.1$) region and, consequently, had high acceptance for exclusive low multiplicity processes. Studies of Coulomb production were performed in parallel
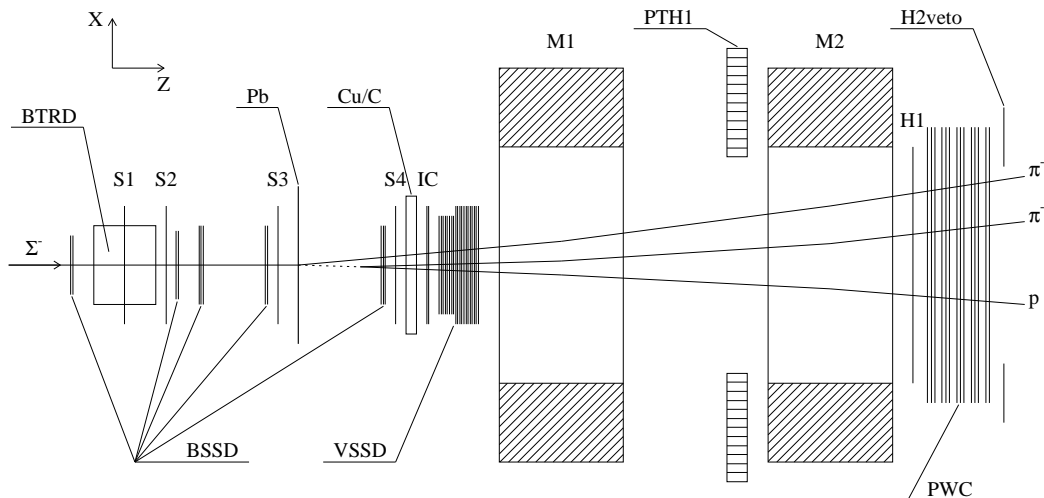
4

Fig. 1. Schematic plan view (not to scale) of the SELEX apparatus. Shown are major detectors used for these measurements: BTRD — beam transition radiation detector; BSSD — beam silicon strip detector; VSSD — vertex silicon strip detectors; PWC — proportional wire chambers; M1, M2 — analyzing magnets; Pb — target for this measurement; Cu/C — targets for charm production measurements; S1–S4, IC — scintillation counters; H1, H2veto — trigger hodoscope and veto; PHT1 — lead glass photon detector.

with the main charm-physics program and several other measurements. This imposed certain limitations on the trigger, geometry, choice of targets and consequent statistics.

We report studies based on a special short exposure with a thin ($1.98\,\mathrm{mm}$) Pb target. Figure 1 shows a portion of the SELEX apparatus relevant for this measurement. The origin of the coordinate system was chosen to be in the middle of the downstream surface of the downstream target, and the Z-axis was directed along the beam. The Pb target was located at $Z = -55\,\mathrm{cm}$, while standard targets for charm measurements were removed for most of the exposure. At the position of the Pb target, the beam was composed of $\approx 50\%\ \pi^-$, $\approx 48\%\ \Sigma^-$ and $\approx 1\%\ \Xi^-$. Fractions of $\bar{p}$ and Ω^- were estimated to be less than 0.1%. The beam transition-radiation detector provided reliable separation of baryons from π^-. Silicon strip detectors (most of which had $4\,\mu\mathrm{m}$ transverse position resolution) provided parameters of the beam and secondary tracks in the target region. After deflection by analyzing magnets, tracks were measured in 14 planes of $2\,\mathrm{mm}$ proportional wire chambers. The absolute momentum scale was calibrated using the $K_S^0 \to \pi^+\pi^-$ decays. Mass resolution in the $\Sigma(1385)$ region was measured using the beam $\Xi^- \to \Lambda\pi^-$ decays, and was found to be $\approx 6\,\mathrm{MeV}$.

Reaction (2) was singled out with the help of a special exclusive trigger. This trigger used scintillation counters S1–S4 to define beam time, and trigger

hodoscope H1 to require three charged tracks. Pulse heights in the scintillation counters IC were used to select three charged tracks, while pulse heights in counters S2 and S3 were used to suppress interactions initiated upstream of the Pb target. Thus, the trigger limited the decay volume of the Λ to the region between the S3 and IC counters, or from $-68\,\mathrm{cm}$ to $2.5\,\mathrm{cm}$ in SELEX coordinates. Finally, to reduce the background trigger rate to an acceptable level, the aperture was limited by veto counters H2veto, which had very little effect on the efficiency for Reaction (2).

A special on-line filter was used to reduce the number of exclusive events written to tape. This selected events that had at least two reconstructed segments downstream of the analyzing magnets. Very loose criteria were imposed on the number of hits in the tracking detectors to reduce processing time. All these requirements were not very restrictive, and are expected to have only minor effect on the process of interest.

3 Data analysis

Events for Reaction (2) were selected by requiring a reconstructed beam track and three charged tracks in the final state, of which one was positive and two negative. The beam particle had to be identified as a Σ^- (Ξ^-) by the beam transition-radiation detector. There was no explicit identification of the produced particles: a proton mass was assigned to the positive track and a pion mass to each negative track. It was then required that one of the pions and the proton formed a good vertex (referred to as secondary) with an effective mass close to the Λ mass: $1.11\,\mathrm{GeV} < M(p\pi^-) < 1.122\,\mathrm{GeV}$. Then, a primary vertex was formed using the remaining pion, the beam, and the reconstructed Λ tracks. Typical resolution for vertices along the beam direction (Z) was $1\,\mathrm{cm}$. To suppress inclusive ($\Lambda\pi^- + X$) background, the energy sum of the observed particles was required to be within $\pm 20\,\mathrm{GeV}$ ($\approx \pm$ two standard deviations) of the beam energy. For further supression of these events, the most upstream photon detector (PHT1) was used as a guard system, requiring that any registered energy be less than $2\,\mathrm{GeV}$.

Beam $\Xi^- \to \Lambda\pi^-$ decays are also selected by the above-described procedure. Events in which Ξ^- decays took place in the Pb target constitute unavoidable background to the $\Lambda\pi^-$ final state. To study this and all other [17] backgrounds caused by beam-particle decays, two regions were defined for the primary vertex: a target region ($-58\,\mathrm{cm} < Z_{\mathrm{pri}} < -52\,\mathrm{cm}$) and sidebands upstream

---

[17] For example, $\Sigma^- \to n\pi^-$ decay, with subsequent n dissociation in matter into $p\pi^-$, mimics Reaction (2) when the $p\pi^-$ effective mass falls in the Λ window and p_{T}^2 is small.

$(-63\,\text{cm} < Z_\text{pri} < -60\,\text{cm})$ and downstream $(-50\,\text{cm} < Z_\text{pri} < -47\,\text{cm})$ of it. Secondary vertex selection $Z_\text{sec} > -45\,\text{cm}$ provided equal Λ decay probabilities for each region. The effective mass distribution of the $\Lambda\pi^-$ systems for events with very small values of the square of the transverse momentum $(p_\text{T}^2 < 0.001\,\text{GeV}^2)$, where most of the Coulomb production is concentrated, is shown in Fig. 2. Data for the primary vertex in the target region are shown by the open histogram, and data for sidebands are shown hatched.

A clear Ξ^- peak is seen in the target region. As expected, to within statistical accuracy, the number of Ξ^- decays in the sidebands is the same as in the target region. However, outside of the Ξ^- peak, there are almost no events in the sidebands. Thus, with exception of the $1.305\,\text{GeV}$–$1.340\,\text{GeV}$ region of $\Lambda\pi^-$ mass, events with a primary vertex in the target region are dominated by beam interactions, and background from beam decays is negligible.

Although it is possible to subtract the background using the sideband regions,
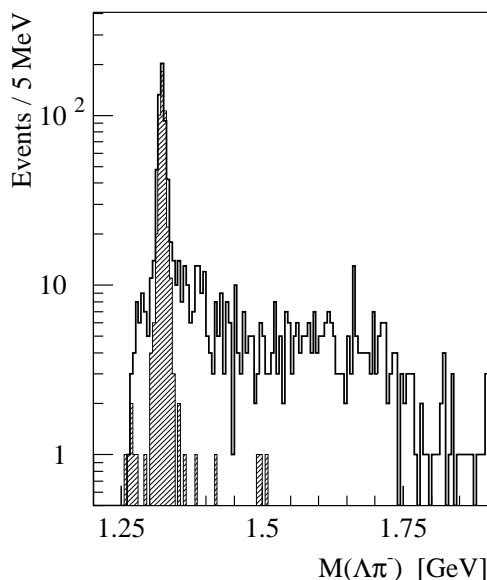

Fig. 2. $M(\Lambda\pi^-)$ distributions for $p_\text{T}^2 < 0.001\,\text{GeV}^2$. Events with a primary vertex in the target region are shown by the solid line, and events corresponding to sidebands are shown hatched.
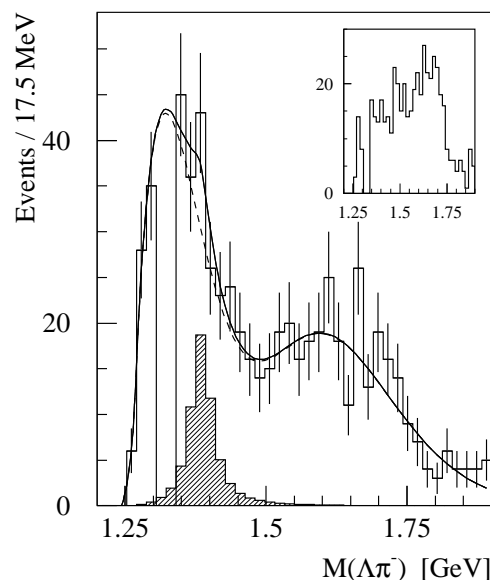
Fig. 3. $M(\Lambda\pi^-)$ distribution for $p_\text{T}^2 < 0.001\,\text{GeV}^2$, ignoring the Ξ^- region in Fig. 2. Example of a fit is shown by the solid line, which includes background for $\Sigma(1385)^-$ Coulomb production (dashed line) and possible signal. The latter is shown by the excess above the dashed line and by the hatched distribution, which corresponds to a derived 90% CL upper limit for the radiative width of the $\Sigma(1385)^-$. The inset shows $M(\Lambda\pi^-)$ distribution for $0.002\,\text{GeV}^2 < p_\text{T}^2 < 0.006\,\text{GeV}^2$.

7

the Ξ^- peak is so dominant that the statistical error on the difference exceeds any signal expected in that region. That is why we decided simply to ignore the region of $1.305\,\mathrm{GeV}$–$1.340\,\mathrm{GeV}$ in our analysis. The resulting distribution (with a secondary vertex selection of $Z > -50\,\mathrm{cm}$, to use the entire decay volume) is shown as the histogram in Fig. 3. There is no clear evidence for $\Sigma(1385)^-$ production, and we use the data to set an upper limit. This requires an absolute normalization of the spectrum in Fig. 3, and a description of the shape and magnitude of any expected signal.

The absolute cross section for the observed $\Lambda\pi^-$ spectrum was determined by making use of the known Σ^-/π^- ratio in the beam, and by normalizing the data relative to similar diffractive $\pi^+\pi^-\pi^-$ production on C and Pb nuclei, and by then using the absolute $\pi^+\pi^-\pi^-$ production cross section on C (see next paragraph). As far as the trigger is concerned, there is no difference between the previously studied three-pion production on C and Pb targets [25] and $\Lambda\pi^-$ production on the Pb target, provided that the Λ decayed upstream of the IC counters. Main trigger inefficiencies are due to pulse height selection in the IC counters and accidental vetoes. These do not depend on event topology. Thus, in such an analysis, most trigger and all luminosity uncertainties cancel. Remaining differences in efficiencies of the trigger and of further event processing are mainly due to different kinematics. These are corrected using a GEANT-based Monte-Carlo program [26]. In particular, for the $\Lambda\pi^-$ system an angular distribution of $1 + 3\sin^2\theta\sin^2\phi$ is used, as expected for electromagnetically produced $\Sigma(1385)^-$ in assumption of a purely magnetic-dipole transition $\Sigma(1385)^- \to \Sigma^-\gamma$. Due to high ($\sim 70\%$, assuming the Λ decayed in selected region) geometrical acceptance of the SELEX apparatus to relevant processes, systematical uncertainties of the relative normalization are negligible.

In this analysis, the diffractive production cross section refers to the number of events observed in the first diffractive exponential of the p_{T}^2 distribution for events in the $0.8\,\mathrm{GeV} < M(3\pi) < 1.5\,\mathrm{GeV}$ mass range. This was measured in special runs with a so-called "beam" trigger. This trigger employed scintillation counters to define beam particles and to reject halo, and required no information from detectors downstream of the targets. The measured value $\sigma_{\mathrm{diff}}(\mathrm{C}) = 2.57 \pm 0.13\,\mathrm{mb}$ is based therefore on a completely unbiased set of interactions. More detailed information on absolute normalization procedures can be found in our previous publication [25].

The differential cross section for the $\Lambda\pi^-$ Coulomb production by Σ^- is given by the expression [27, 28]:

$$\frac{\mathrm{d}\sigma}{\mathrm{d}M\,\mathrm{d}q^2} = \frac{2\alpha}{\pi} Z^2 \frac{M}{M^2 - m_{\Sigma^-}^2}\, \sigma_\gamma(M)\, \frac{q^2 - q_{\min}^2}{q^4} |F(q^2)|^2 \qquad (3)$$

where α is the fine structure constant, Z is the charge of the nucleus, M is the effective mass of the produced system, $\sigma_\gamma(M)$ is the cross section for the reaction $\gamma\Sigma^- \rightarrow \Lambda\pi^-$, q^2 is the square of the momentum transfer, q^2_{min} is its minimal value, and $F(q^2)$ is the nuclear form factor. For the case of photoproduction through the $\Sigma(1385)^-$ resonance (designated in the formulae as Σ^*), the cross section $\sigma_\gamma(M)$ is given by the expression [29]:

$$\sigma_\gamma(M) = 8\pi \frac{M^2}{(M^2 - m^2_{\Sigma^-})^2} \frac{2J_{\Sigma^*}+1}{2J_{\Sigma^-}+1} \frac{m^2_{\Sigma^*}\Gamma(\Sigma^-\gamma)\Gamma(\Lambda\pi^-)}{(M^2 - m^2_{\Sigma^*})^2 + m^2_{\Sigma^*}\Gamma^2_{tot}} \tag{4}$$

where J stands for spin and Γ for partial (and Γ_{tot} for total) width.

The Coulomb form factor $F(q^2)$ in Eq. (3) accounts for the nuclear charge distribution, initial and final state absorption, as well as the Coulomb phase. It was calculated in the framework of the optical model as developed in Ref [30]. This model requires as input the total Σ^--nucleon cross section σ, and the ratio of real to imaginary parts of the forward scattering amplitude (ρ'), at the appropriate beam energy. We used the cross section $\sigma = 37.0\,\text{mb}$ determined in the SELEX experiment, and the extrapolated value of $\rho' = 0.04$ [31]. The impact of these parameters on $F(q^2)$ at our energy and q^2 range is quite minimal.

At high beam energy, q^2_{min} can be approximated by:

$$q^2_{min} \approx (M^2 - m^2_{\Sigma^-})^2/(4P^2_{beam}) \tag{5}$$

For $M \approx 1.385\,\text{GeV}$, q^2_{min} is $\approx 3 \cdot 10^{-7}\,\text{GeV}^2$. Cross section (3) peaks at $q^2 = 2q^2_{min}$, and then falls approximately as $1/q^2$. Thus, the measured transverse momentum distribution is determined mainly by experimental resolution, which was obtained from studies of beam $\Xi^- \rightarrow \Lambda\pi^-$ decays. In particular, since there is no momentum transfer in such decay, the measured distribution directly reflects the resolution. This was found to be Gaussian, with a standard deviation varying from 16.3 to 17.8 MeV, depending on data set and cutoff criteria. Equation (3) was integrated numerically to extract a cross section for $p^2_{\text{T}} < 0.001\,\text{GeV}^2$, to be used for comparison with data.

When describing Primakoff production of the $\Sigma(1385)^-$ resonance, its mass, total width, and branching to $\Lambda\pi^-$ were fixed to their known PDG values [32]. The only fitted parameter was the radiative decay width. Background was described by two smooth functions, vanishing at the $\Lambda\pi^-$ threshold. The first function was

$$f_1(M) = P_1 (M - M_{thr})^{P_2} \exp\left[-P_3(M - M_{thr})\right] \tag{6}$$

where M_{thr} was threshold mass, and P_i were free parameters. This function qualitatively described mass spectrum in the region $M < 1.5\,\mathrm{GeV}$. The second function, capable of describing the entire mass spectrum, was

$$
\begin{aligned}
f_2(M) = {} & P_1\,(M - M_{\mathrm{thr}})^{P_2}\,\exp\left[-P_3(M - M_{\mathrm{thr}})\right] \\
& + P_4\,(M - M_{\mathrm{thr}})^{P_5}\,\exp\left[-P_6(M - M_{\mathrm{thr}})\right]
\end{aligned}
\tag{7}
$$

We made fits using the whole data set, and using a reduced data set where charm targets were absent, and, in particular, p_{T} resolution was better. There are arguments in favour of using for final analysis each of these data sets, so we quote an average. The difference is minor anycase. Results of the fits and derived upper limits are summarized in Table 1. An example of a fit (function f_2, first line in Table 1) is shown in Fig. 3. The fits showed no significant changes for small variations in selection criteria and histogram binning. However, significant uncertainty is associated with background description. When giving an upper limit, there is no conventional way of dealing with such type of uncertainty. It was taken into account by using the worst case of function f_2.

Data set	$\Gamma^{(1)}_{\mathrm{fit}}$	$\Gamma^{(1)}_{90\%}$	$\Gamma^{(2)}_{\mathrm{fit}}$	$\Gamma^{(2)}_{90\%}$
All data	0.37 ± 3.79	6.5	3.66 ± 4.36	9.8
Without charm targets	-1.99 ± 4.42	6.2	1.32 ± 5.08	9.2

Table 1
Results of the fits for $\Gamma(\Sigma^-\gamma)$ and derived upper limits (everything in keV).

We quote an upper limit at the 90% confidence level, which includes all sources of uncertainty, as:

$$
\Gamma\left[\Sigma(1385)^- \to \Sigma^-\gamma\right] < 9.5\,\mathrm{keV}
\tag{8}
$$

Our result is dominated by statistical uncertainty and uncertainty, associated with background description. Other systematics uncertainties include absolute normalization (5%), transverse momentum resolution (1.8%), accuracy of $F(q^2)$ (1%), and uncertainties in the PDG parameters of the $\Sigma(1385)^-$ resonant mass (1%), width (5%), and branching to $\Lambda\pi^-$ (2%). Added in quadrature, these do not exceed 8%. The hatched distribution in Fig. 3 shows what the signal spectrum would look like, given the limit in Eq. (8).

It is interesting to investigate what mechanism is responsible for producing the $\Lambda\pi^-$ system shown in Fig. 3. To do this, a $\Lambda\pi^-$ mass distribution was studied for the $0.002\,\mathrm{GeV}^2 < p_{\mathrm{T}}^2 < 0.006\,\mathrm{GeV}^2$ range (see the inset in Fig. 3), which is almost free of Coulomb contribution, and which is expected to be dominated by diffractive production. The enhancement in Fig. 3 in the region of $M \lesssim 1.45\,\mathrm{GeV}$ is not present at higher transverse momenta. This suggests

an electromagnetic origin. To check this, the p_T^2 distributions were studied for mass regions below and above 1.45 GeV. Both distributions showed strong forward peaking behavior, which could be described by falling exponential $\exp(-bp_\mathrm{T}^2)$. For $M > 1.45\,\mathrm{GeV}$ we obtained the slope $b \simeq 400\,\mathrm{GeV}^{-2}$, a value typical for diffractive production on the Pb nucleus, but for $M < 1.45\,\mathrm{GeV}$, we obtained a slope $b \simeq 1000 \pm 100\,\mathrm{GeV}^{-2}$. This is too steep to be explained by diffraction, but quite reasonable assuming a significant Coulomb contribution. Thus we conclude that $M \lesssim 1.45\,\mathrm{GeV}$ region is dominated by electromagnetic production. Using Eq. (3), it is then possible to derive a cross section for the reaction

$$\gamma\Sigma^- \to \Lambda\pi^- \tag{9}$$

Available data do not allow us to separate Coulomb and strong production mechanisms very precisely. Also, there is an uncertainty in $\Lambda\pi^-$ detection efficiency, since angular distribution of that system is not given by theory. We estimate the cross section of Reaction (9), including any possible $\Sigma(1385)^-$ resonant production, to be

$$\sigma\big[\gamma\Sigma^- \to \Lambda\pi^-\big]\Big|_{\sqrt{s}\approx 1.385\,\mathrm{GeV}} = 56 \pm 12 \pm 11\,\mu\mathrm{b} \tag{10}$$

Factors, contributing to systematical uncertainty, include absolute normalization (5%), transverse momentum resolution (1.8%), strong production (10%), and $\Lambda\pi^-$ detection efficiency (15%).

The fact that electromagnetic production dominates at low effective masses M is not surprising, given the factor $M/(M^2 - m_{\Sigma^-}^2)$ in the cross section of Eq. (3).

4   Discussion

The upper limit of 9.5 keV at 90% confidence level, obtained for $\Gamma[\Sigma(1385)^- \to \Sigma^-\gamma]$, is the best measurement to date, and improves by a factor of 2.5 the only previous limit of 24 keV [4]. The current limit falls just at the edge of the range of theoretical predictions [6, 7, 8, 9, 10, 11, 12, 13, 14, 15, 16, 17, 18, 19].

As far as we know, the result in Eq. (10) is the first experimental measurement of photoproduction on Σ^-. We are not aware of any theoretical calculations for this value. In view of this result, it is interesting to discuss prospects for a new $\Sigma(1385)^- \to \Sigma^-\gamma$ measurement. Using Eq. (4), the dependence between the cross section for resonance photoproduction at the $\Sigma(1385)^-$ pole and the radiative width of this resonance can be expressed numerically as $\sigma_\gamma = 3.5\,\mu\mathrm{b/keV} \times \Gamma_\mathrm{rad}$. For Γ_rad in the predicted range, the resonant cross section

is small compared to the total of $56\,\mu$b. Thus, a measurement of the radiative width will require a more sensitive experiment by an order of magnitude if $\Gamma_{\rm rad} \approx 4\,{\rm keV}$, or by two orders of magnitude if $\Gamma_{\rm rad} \approx 1\,{\rm keV}$.

Finally, we comment on a previous measurement [4]. In that experiment, the upper limit of $24\,{\rm keV}$ was based on 2 events observed in the $\Lambda\pi^-$ spectrum in the $1.375\,{\rm GeV} < M < 1.405\,{\rm GeV}$ mass range, and correspond to at most 5 events at 90% CL [4]. We have a factor of ≈ 30 more $\Lambda\pi^-$ events in that mass range, while our upper limit is only 2.5 times lower. This is because an upper limit is determined mainly by the statistical uncertainties of the electromagnetic nonresonant component in $\Lambda\pi^-$ production. Using our value in Eq. (10) for the $\Lambda\pi^-$ photoproduction cross section, we predict 4.0 ± 1.2 events from Coulomb production in the spectrum of Ref. [4]. Of course, there should also be a contribution from strong production. Still, two detected events seems to be a credible fluctuation down from an extrapolation of our result.

Acknowledgements

References

[1] L. G. Landsberg, Phys. Rept. 128 (1985) 301;
     M. Zielinski, Acta Phys. Pol. B18 (1987) 455.
[2] B. Krusche and S. Schadmand, Prog. Part. Nucl. Phys. 51 (2003) 399;
     V. D. Burkert, Int. J. Mod. Phys. E1 (1992) 421.
[3] L. G. Landsberg, Phys. Atomic Nuclei 59 (1996) 2080.

[4] E. Arik et al., Phys. Rev. Lett. 38 (1977) 1000.

[5] J. Colas, C. Farwell, A. Ferrer and J. Six, Nucl. Phys. B91 (1975) 253.

[6] H. J. Lipkin, Phys. Rev. D7 (1973) 846.

[7] H. J. Lipkin, M. A. Moinester, Phys. Lett. B287 (1992) 179.

[8] A. I. Akhiezer, M. P. Rekalo, JETP Letters 1 (1965) 29.

[9] J. W. Darewych, M. Horbatsch, R. Koniuk, Phys. Rev. D28 (1983) 1125.

[10] R. H. Hackman, N. G. Deshpande, D. A. Dicus, V. L. Teplitz, Phys. Rev. D18 (1978) 2537.

[11] C. L. Schat, C. Gobbi, N. N. Scoccola, Phys. Lett. B356 (1995) 1.

[12] A. Abada, H. Weigel, H. Reinhardt, Phys. Lett. B366 (1996) 26.

[13] T. Haberichter, H. Reinhardt, N. N. Scoccola, H. Weigel, Nucl. Phys. A615 (1997) 291.

[14] M. N. Butler, M. J. Savage, R. P. Springer, Nucl. Phys. B399 (1993) 69.

[15] M. Napsuciale, J. L. Lucio, Nucl. Phys. B494 (1997) 260.

[16] D. B. Leinweber, T. Draper, R. M. Woloshyn, Phys. Rev. D48 (1993) 2230.

[17] R. K. Sahoo, A. R. Panda, A. Nath, Phys. Rev. D52 (1995) 4099.

[18] G. Wagner, A. J. Buchmann, A. Faessler, Phys. Rev. C58 (1998) 1745.

[19] G. Wagner, A. J. Buchmann, A. Faessler, J. Phys. G26 (2000) 267.

[20] H. Primakoff, Phys. Rev. 81 (1951) 899.

[21] I. Pomeranchuk, I. Shmushkevich, Nucl. Phys. 23 (1961) 452.

[22] T. Ferbel, Acta Phys. Pol. B12 (1981) 1129;
M. Zielinski, Acta Phys. Pol. B18 (1987) 455;
L. Landsberg, Phys. Atomic Nuclei 63 (2000) 1.

[23] V. J. Smith, in: S.-U. Chung, H. Willutzki (Eds.), Proc, of the 7th International Conference on Hadron Spectroscopy (HADRON-97), 1997, p. 627.

[24] J. Russ, Nucl. Phys. A585 (1995) 39;
J. Russ et al., in: Proc. of the 29th International Conference on High Energy Physics, 1999, p. 1259, hep-ex/9812031.

[25] V. V. Molchanov et al., Phys. Lett. B521 (2001) 171.

[26] G. Davidenko et al., GE781: A Monte Carlo package for fixed target experiments, in: Proc. of the International Conference on Computing in High Energy Physics'95, September, 1995, p. 832.

[27] A. Halprin, C. Andersen, H. Primakoff, Phys. Rev. 152 (1966) 1295.

[28] G. Fäldt, Nucl. Phys. B43 (1972) 591.

[29] J. D. Jackson, Nuovo Cimento 34 (1964) 1644.

[30] C. Bemporad et al., Nucl. Phys. B51 (1973) 1.

[31] U. Dersch et al., Nucl. Phys. B579 (2000) 277.

[32] K. Hagiwara et al., Phys. Rev. D66 (2002) 010001.